

Supporting Information

Molecular engineering of anthracene-based emitters for highly efficient nondoped deep-blue fluorescent OLEDs

Yaxiong Wang,^a Wei Liu,^{a,b} Shaofeng Ye,^a Qing Zhang,^a Yalei Duan,^a Runda Guo,^{*a} and Lei Wang^{*a}

^a Wuhan National Laboratory for Optoelectronics, Huazhong University of Science and Technology, Wuhan, 430074, People's Republic of China.

^b Institute for smart Materials & Engineering, University of Jinan, No. 336 Nanxinzhuan west Road, Jinan 250022, People's Republic of China.

*Email: wanglei@mail.hust.edu.cn, runda_guo@hust.edu.cn.

Contents

1. **Fig. S1.** The ¹H NMR spectra of *pCzphAnBzt*.
2. **Fig. S2.** The ¹³C NMR spectra of *pCzphAnBzt*.
3. **Fig. S3.** The ¹H NMR spectra of *mCzAnBzt*.
4. **Fig. S4.** The ¹³C NMR spectra of *mCzAnBzt*.
5. **Fig. S5.** The ¹H NMR spectra of *m2CzAnBzt*.
6. **Fig. S6.** The ¹³C NMR spectra of *m2CzAnBzt*.
7. **Fig. S7.** The normalized UV-vis spectra and normalized PL spectra of *pCzphAnBzt* in different solvents.
8. **Fig. S8.** The normalized UV-vis spectra and normalized PL spectra of *mCzAnBzt* in different solvents.
9. **Fig. S9.** The normalized UV-vis spectra and normalized PL spectra of *m2CzAnBzt* in different solvents.
10. **Table S1.** Detailed information of absorption and emission peak positions of *pCzphAnBzt*, *mCzAnBzt*, *m2CzAnBzt* in different solvents.
11. **Fig. S10.** Cyclic voltammetry scans of *pCzPhAnBzt*, *mCzAnBzt* and *m2CzAnBzt*.
12. **Fig. S11.** Normalized EL spectra of *pCzAnBzt* and *pCzphAnBzt* at 6 V.
13. **Fig. S12.** The hole-only and electron-only devices of *pCzPhAnBzt*-, *mCzAnBzt*- and *m2CzAnBzt*-based nondoped device.
14. **Fig. S13.** Amplified EL decay of the delayed component of *pCzPhAnBzt*-, *mCzAnBzt*- and *m2CzAnBzt*-based nondoped device at 5V.
15. **Fig. S14.** Transient EL decays of *pCzAnBzt* nondoped devices at 5 V.
16. **Table S2.** Optical parameters of *pCzAnBzt*, *pCzphAnBzt*, *mCzAnBzt* and *m2CzAnBzt*-based nondoped devices calculated by transient EL decays at 5V voltage.

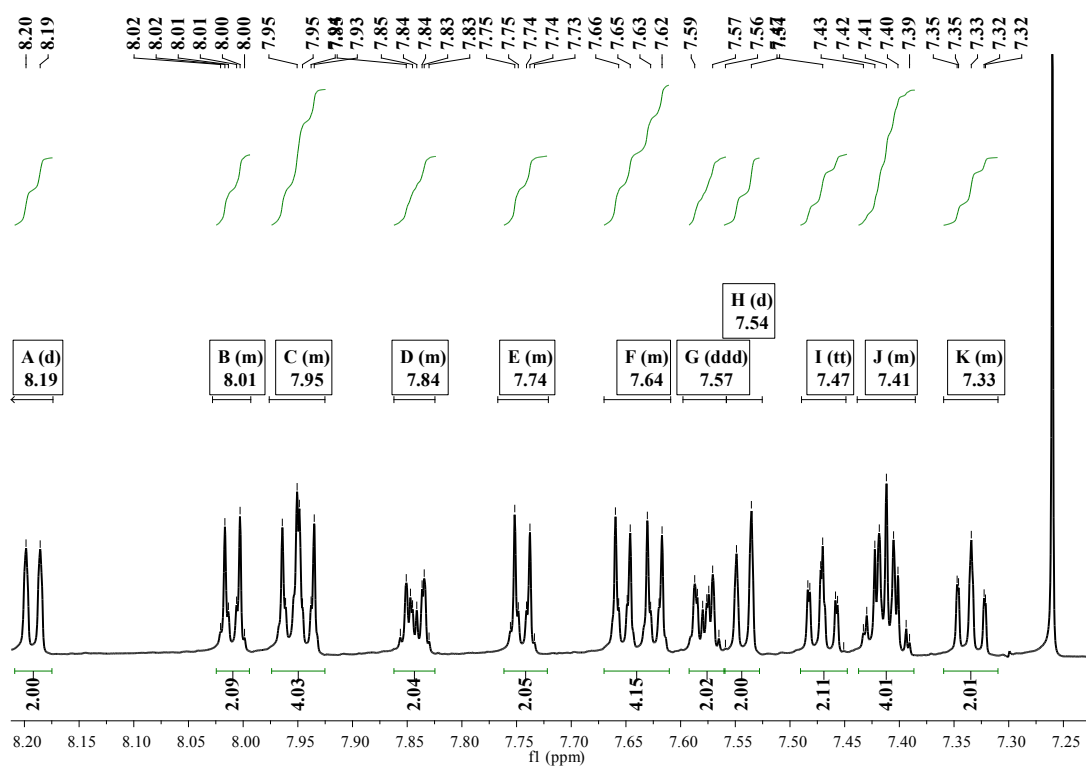


Fig. S1. The ^1H NMR spectra of *pCzphAnBzt*

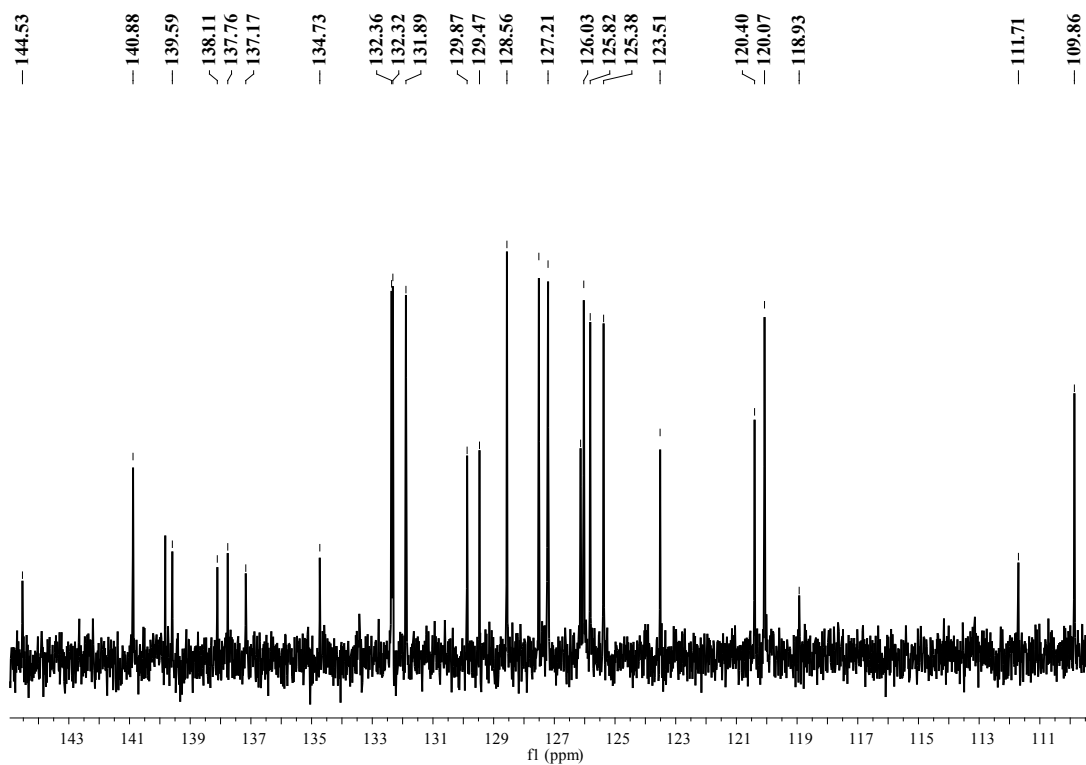


Fig. S2. The ^{13}C NMR spectra of *pCzphAnBzt*.

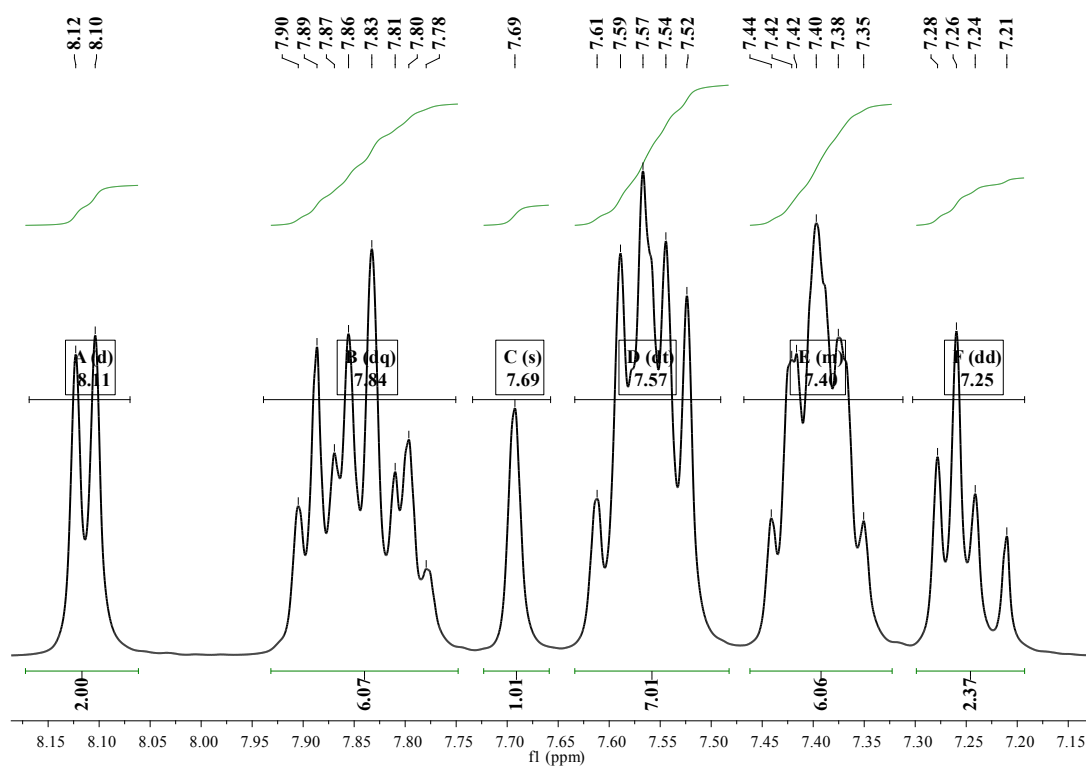


Fig. S3. The ^1H NMR spectra of *mCzAnBzt*.

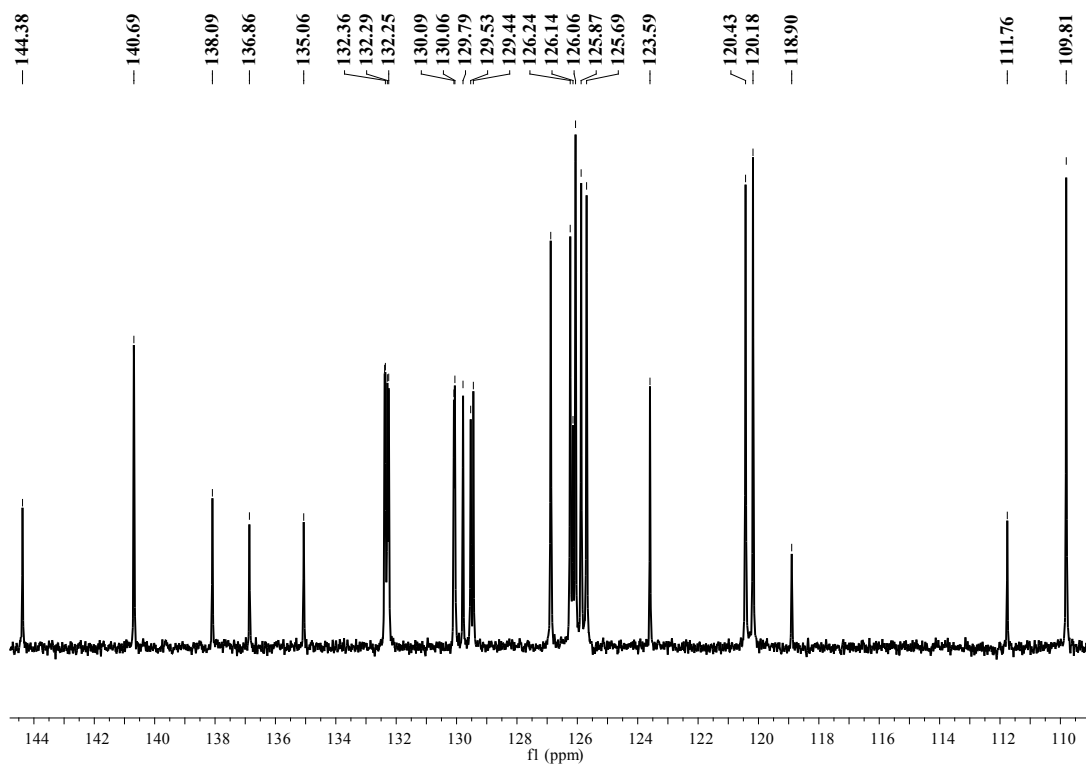


Fig. S4. The ^{13}C NMR spectra of *mCzAnBzt*.

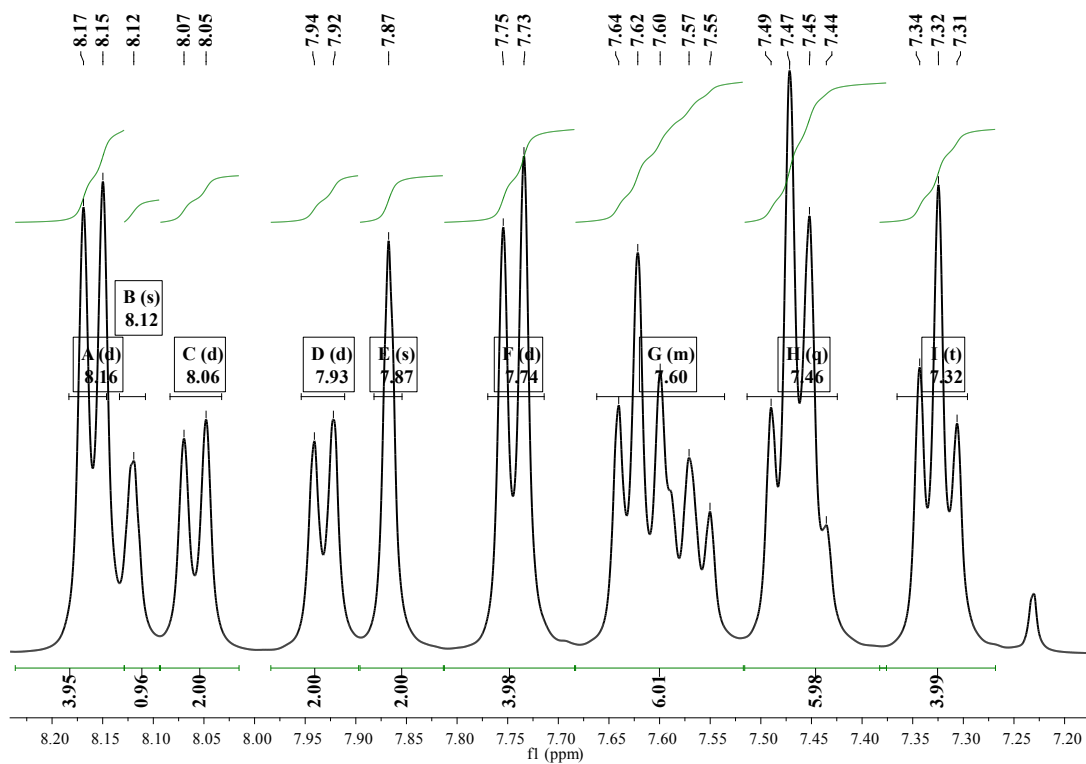


Fig. S5. The ^1H NMR spectra of *m2CzAnBzt*.

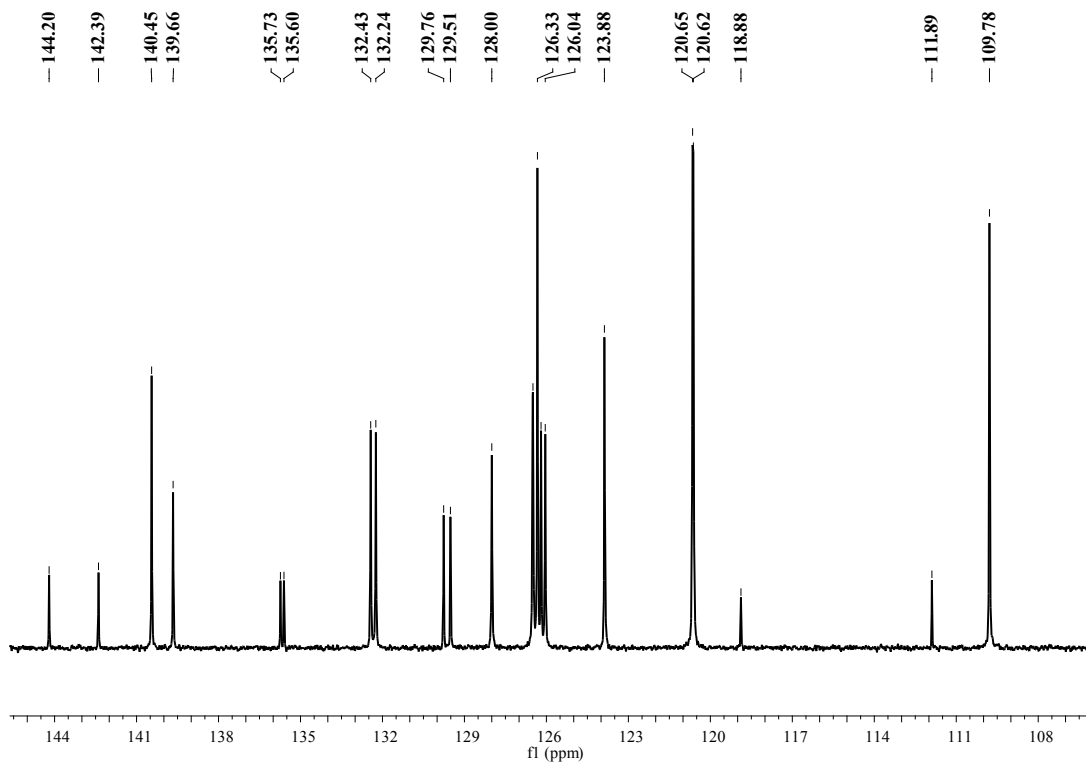


Fig. S6. The ^{13}C NMR spectra of *m2CzAnBzt*.

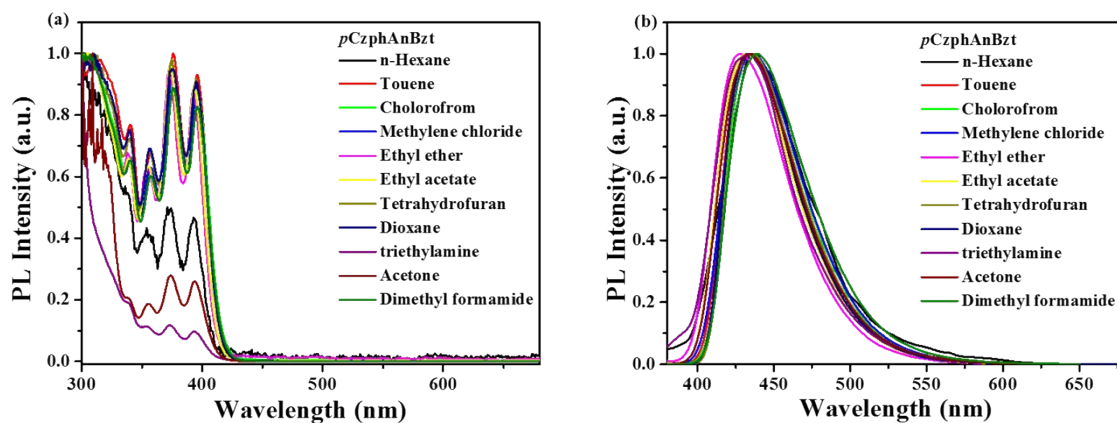


Fig. S7. The normalized UV-vis spectra (a) and normalized PL spectra (b) of *pCzphAnBzt* in different solvents.

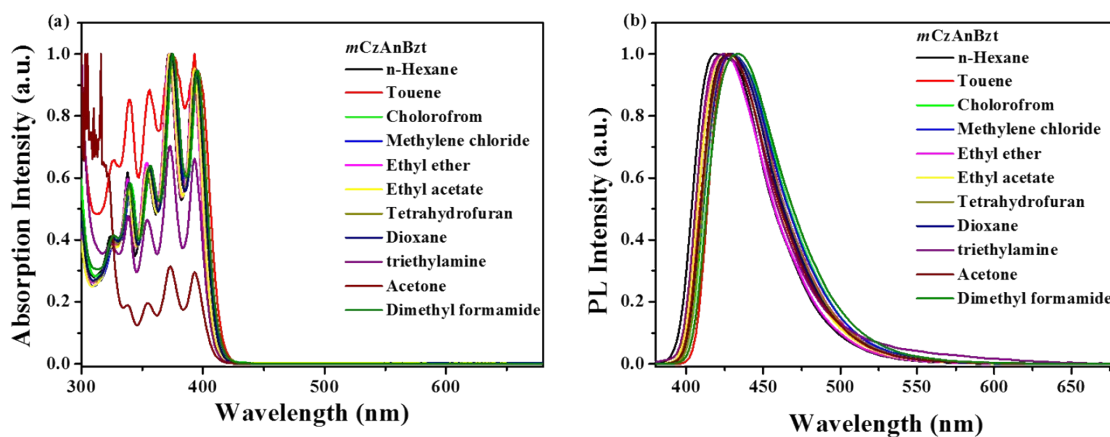


Fig. S8. The normalized UV-vis spectra (a) and normalized PL spectra (b) of *mCzAnBzt* in different solvents.

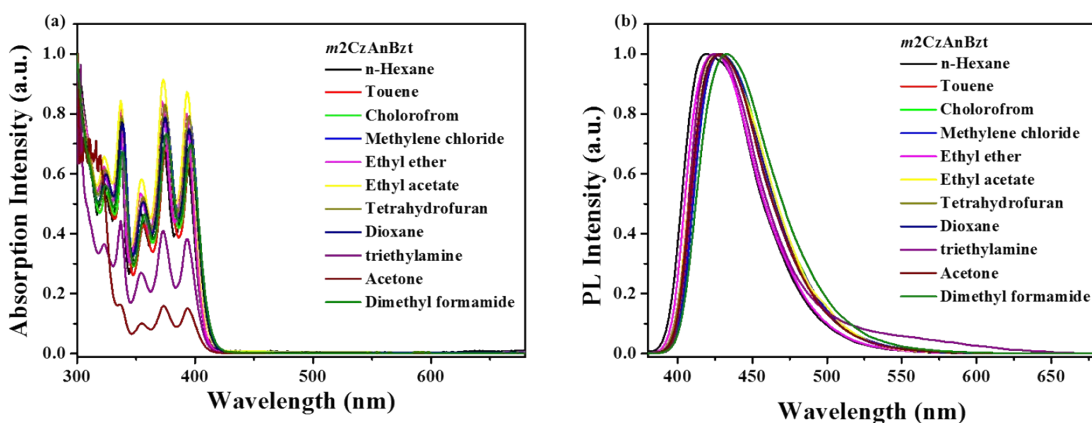


Fig. S9. The normalized UV-vis spectra (a) and normalized PL spectra (b) of *m2CzAnBzt* in different solvents.

Table S1. Detailed information of absorption and emission peak positions of *pCzphAnBzt*, *mCzAnBzt* and *m2CzAnBzt* in different solvents.

Solvent	<i>pCzphAnBzt</i>		<i>mCzAnBzt</i>		<i>m2CzAnBzt</i>	
	λ_a (nm)	λ_f (nm)	λ_a (nm)	λ_f (nm)	λ_a (nm)	λ_f (nm)
Hexane	393	436	392	418	392	420
Touene	396	433	393	430	396	428
Choloroform	396	436	396	430	396	428
Methylene chloride	396	437	395	430	395	428
Ethyl ether	393	428	392	424	393	424
Ethyl acetate	393	432	393	426	393	428
Tetrahydrofuran	395	436	394	428	395	428
Dioxane	395	432	395	428	395	428
Triethylamine	393	434	393	424	393	424
Acetone	394	435	393	428	394	428
Dimethyl formamide	396	439	395	434	396	432

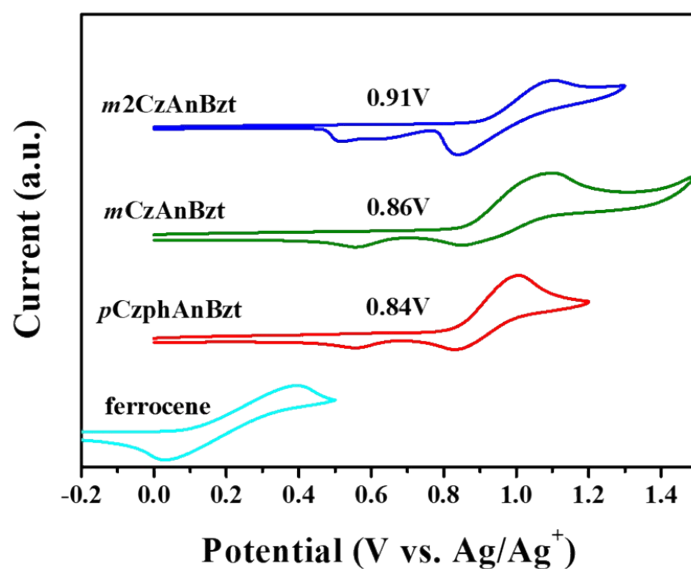


Fig. S10. Cyclic voltammety scans of *pCzPhAnBzt*, *mCzAnBzt* and *m2CzAnBzt*.

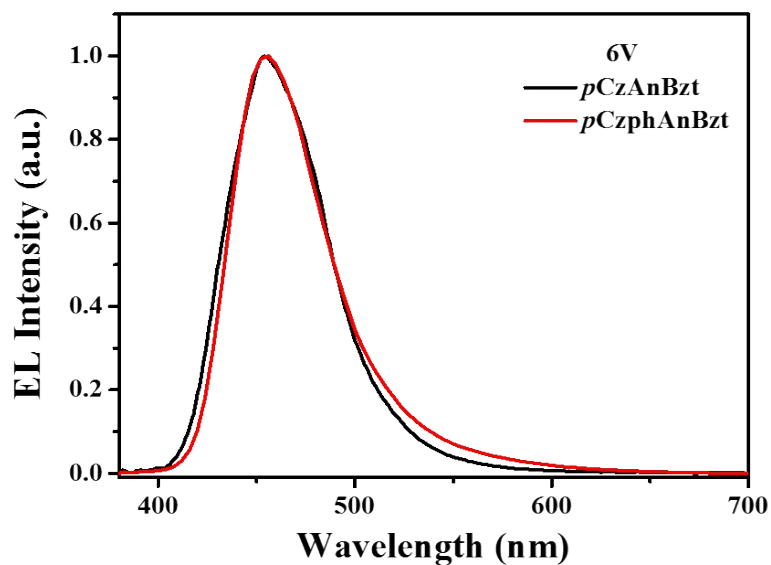


Fig. S11. Normalized EL spectra of *pCzAnBzt* and *pCzphAnBzt* at 6 V.

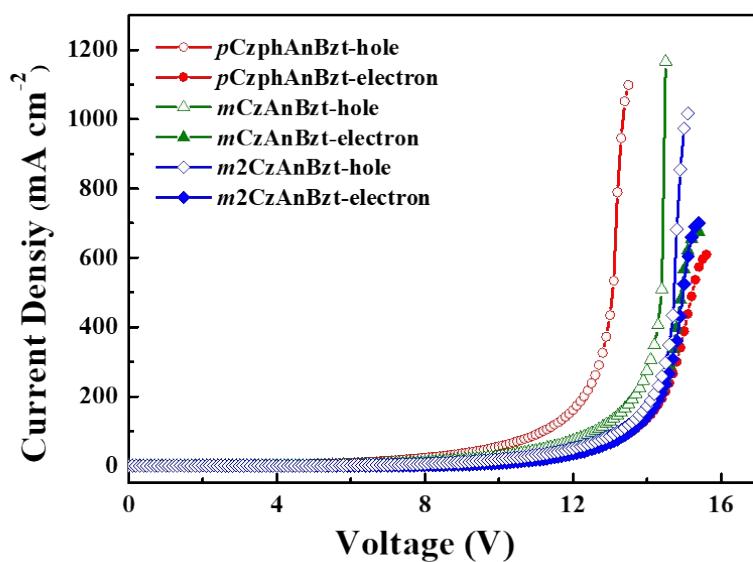


Fig. S12. The hole-only and electron-only devices of *pCzPhAnBzt*-, *mCzAnBzt*- and *m2CzAnBzt*-based nondoped device. The devices structure of hole-only: ITO/HATCN (15 nm)/TAPC (50 nm)/TCTA (5 nm)/EML (20 nm)/TCTA (5 nm)/TAPC (50 nm)/HATCN (15 nm)/Al(150 nm), and the devices structure of electron-only: ITO/LiF(1 nm)/TmPyPB (40 nm)/EML (20 nm)/TmPyPB (40 nm)/LiF(1 nm)/Al(150 nm).

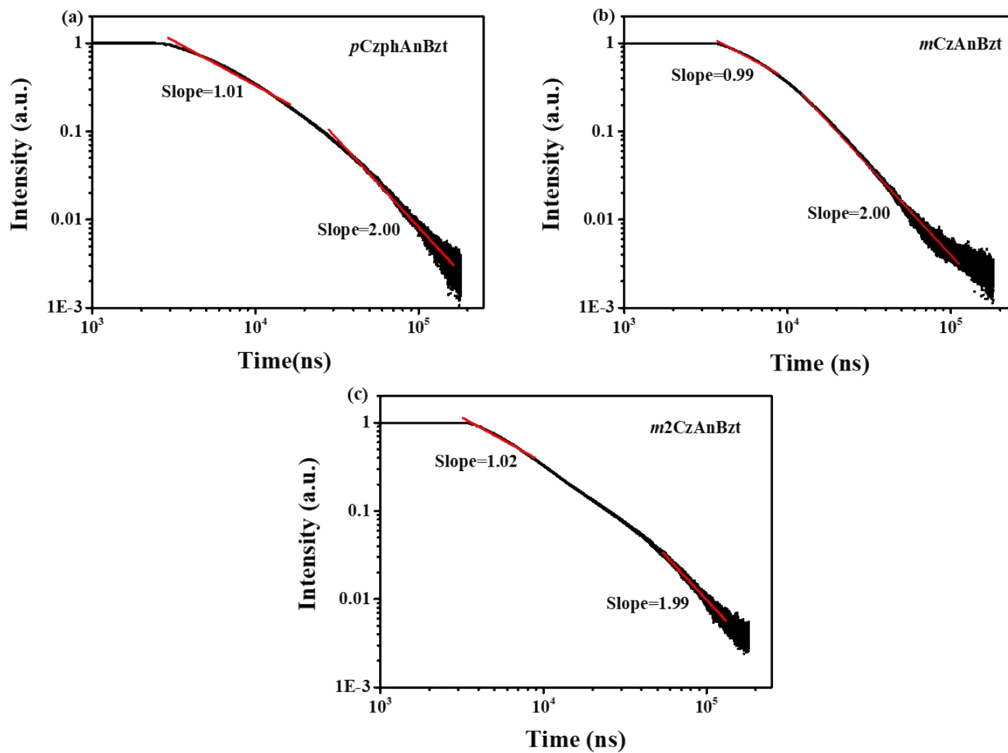


Fig. S13. Amplified EL decay of the delayed component of *pCzPhAnBzt*-, *mCzAnBzt*- and *m2CzAnBzt*-based nondoped device at 5V.

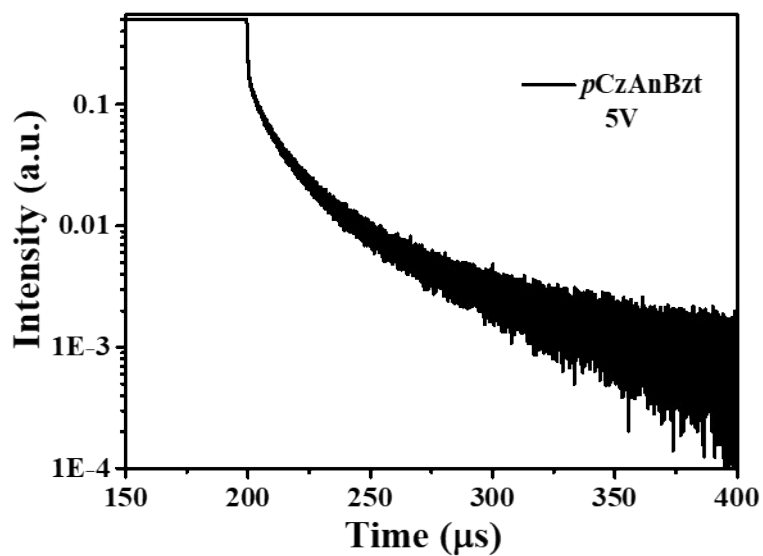


Fig. S14. Transient EL decays of *pCzAnBzt*-based nondoped devices at 5 V.

Table S2. Optical parameters of *pCzAnBzt*-, *pCzphAnBzt*-, *mCzAnBzt*- and *m2CzAnBzt*-based nondoped devices calculated by transient EL decays at 5V voltage.

compound	$I_{\text{delay}}/I_{\text{steady}}$	$\eta_{\text{TTA}}^{\text{a}}$	$\eta_{\text{rad}}^{\text{b}}$	$\text{EQE}_{\text{ca}}^{\text{c}}(\%)$	$\text{EQE}_{\text{ex}}^{\text{d}}(\%)$
<i>pCzAnBzt</i>	0.4096	0.1734	0.4234	7.53	9.23
<i>pCzphAnBzt</i>	0.2980	0.1061	0.3561	3.63	6.75
<i>mCzAnBzt</i>	0.1977	0.0616	0.3116	5.89	7.95
<i>m2CzAnBzt</i>	0.3228	0.1192	0.3692	5.87	7.36

^a Exciton utilization by TTA process. ^b Total ratio of radiative excitons. ^c EQE calculated using equation $\text{EQE} = (\gamma \times \eta_{\text{rad}} \times \Phi_{\text{PL}}) \eta_{\text{out}}$, assuming $r=1$, $\eta_{\text{out}}=0.3$. ^d Experiment value.